Modelling Foveated Depth-of-field Blur for Improving Depth Perception in Virtual Reality

Razeen Hussain
University of Genoa
Genoa, Italy
razeen.hussain@edu.unige.it

Manuela Chessa
University of Genoa
Genoa, Italy
manuela.chessa@unige.it

Fabio Solari
University of Genoa
Genoa, Italy
fabio.solari@unige.it

2020 IEEE 4th International Conference on Image Processing, Applications and Systems (IPAS) | 978-1-7281-7574-4/20/$31.00 ©2020 IEEE | DOI: 10.1109/IPAS50080.2020.9334947

***Abstract*—This paper presents a technique to incorporate spatial blur effects in virtual reality devices. The considered spatial blur is based on foveation and defocus blur: concepts inspired by the human visual system. The proposed technique can be applied to any head-mounted display as a post-processing step. Our foveated depth-of-field method removes intensity leakage artifacts in the transitory regions and works in real-time. We verify the usefulness of our technique by conducting a pilot study on depth perception in virtual environments. In the conducted user study, systems integrated with our blur effect provided a better estimation of object depth in the peripheral regions.**

***Index Terms*—foveation, depth-of-field, shader, gaze contingency, depth perception, image processing**

I. Introduction

Virtual reality (VR) is an emerging field with applications in numerous sectors such as education, health, military, and training. Modern head-mounted displays (HMDs), although much advanced, are still unable to provide a visual experience similar to the real world experience. These devices present the virtual environment in pin-sharp focus as they aim to allow the user to extract information from all areas of the projected images [1]. This causes visual fatigue or simulator sickness and is in contrast to the natural viewing of humans in the real world. Humans continuously change their eye position and accommodation in order to focus at different objects in their surroundings. All objects placed at the accommodative distance tend to form a sharp image on the retinae while all other objects appear out-of-focus [2]. This phenomena is referred to as depth-of-field (DoF) effects in computer graphics. Incorporating spatial blur or defocus blur, while providing stereoscopic 3D stimuli has shown to reduce visual fatigue [3], [4]. Moreover, defocus blur can be used to highlight specific portions of the scene [5].

Foveated imaging is a technique in which the image resolution varies across the image according to the fixation point. This technique aims to simulate a drop in acuity in the visual system from fovea to periphery, as experienced by humans, by rendering peripheral content to a smaller frame buffer resolution and then resampling it using a range of temporal and spatial upscaling algorithms [6]. Recent developments in the field of foveated rendering [7]–[9] has helped reduce the computational load for VR devices. Such systems are able to reduce the required number of processed pixels up to 20x and can offer approximately 3x faster rendering times. Although these techniques are able to reduce visual fatigue, but they provide focus information uncoupled from depth information. By using a combination of the two, a more natural scene can be produced [10]. Moreover, a recent work [11] shows that foveation can affect human depth perception.

In VR, spatial blur techniques can be classified into two categories, namely object space and image space methods. Object space methods tend to have more accurate results and suffer less from artifacts as compared to image space methods. However, image space methods are much faster. Speed is of critical importance in VR applications so image space methods are usually preferred. Image space methods need to be tuned carefully to avoid artifacts such as intensity leakage and depth discontinuity. These artifacts mainly occur when there is an abrupt change in the depth map. Based on the current generation HMDs' specifications, human visual system is sensitive to artifacts within 20° of eccentricity [12].

In this paper, we develop a system that takes its inspiration from foveated rendering and DoF rendering. The proposed system aims to couple the output of both approaches and provides an artifact free scene in the foveal region. Our system works in real-time and offers a smooth transition when user's fixation point changes. The novelty of our system is that it combines foveation and DoF blur in a real-time gaze-contingent application for off-the-shelf HMDs. All techniques currently present in the literature for VR/AR focused spatial blur either have a predetermined focus distance (not being fully gaze-contingent) or suffer heavily from artifacts and flickering.

The paper is organized as follows: Section II presents the related works. In Section III, we describe our developed system. Section IV describes an experimental study we conducted to analyse the performance of our system. In Section V, we conclude the paper with a discussion.

II. Related Work

A gaze-contingent system with adaptive focus has been designed recently [13]. The system makes use of adjustable lens that can change the lens properties depending on where the user is looking. The authors argue that such systems have the potential of correcting myopia and hyperopia in VR systems. Similar approaches have also been proposed for VR/AR devices [14]. However, these are hardware intensive and due to lack of affordable and compact focus-tunable lenses, the hardware can not be installed on modern lightweight HMDs.

Phase-aligned approaches for foveated rendering have been proposed recently [15]. The system ensures that each low acuity pixel is aligned with the virtual world rather than the display while only the high acuity regions align with the head movement. Only the foveal regions require additional processing in each frame, however, this approach suffers from flickering when the user produces translational movements.

DoF blur effects have also been implemented for VR/AR [16]. They assume a focus distance for each user and base the blur of each pixel on the depth difference of that particular pixel to the focus distance. Their system does not incorporate an eye tracking system and the focus distance cannot be modified in real-time.

Another approach for DoF blur uses the lens model to compute the circle of confusion (CoC) [17]. They compared user performance between full fidelity and DoF blur conditions in first-person shooter (FPS) games. Their system assumes that the user is always looking at the center of the scene and cannot adapt to other fixation points. Unity 3D[1] game engine's post-processing stack uses a similar approach. However, it does not support VR/AR devices yet and the focus distance is fixed apriori.

There have been some attempts to combine foveated rendering and DoF blur [18], [19]. Their systems suffered from artifacts introduced by DoF filters which are scene dependant. However, they highlighted the need to combine foveated rendering and DoF blur techniques to obtain optimal results.

III. Methodology

The overall system is composed of two types of blur, namely multi-region foveation and DoF effects. All processing is done pixel-wise in the linear colour space at the shader level using image space methods in order to have real-time performance. For the smoothing effect, two types of filter were considered, namely the Gaussian filter and the Bokeh/disc filter. The disc blur corresponds better to the shape of the aperture/pupil present in human eyes and is more realistic. Thus, it is used in the implementation.

A four-pass shader was used to implement the spatial filters. In the first pass, two parameters are computed for each pixel in the frame: the CoC value and the radius from the fixation point. The CoC values are used for the DoF effects while the radii are used for the multi-region foveation. In the second and third passes, the DoF blur and foveation effects are applied respectively to the source image and stored in temporary buffers. In the final pass, the data from the previous two passes is used to compute the final output. The blur effects are created at half resolution of the source image and are upsampled at the end. Fig. 1 highlights the overall process while the details of each shader pass are described below.

[1]http://www.unity.com

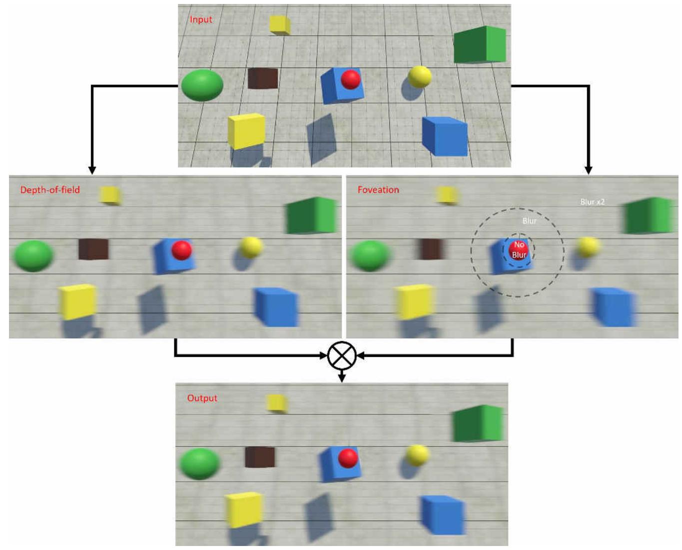

Fig. 1. Example usage of the foveated DoF effects. Top image is the source image. Middle left image is the output of the second shader pass. Middle right image is the output of the third shader pass. Bottom image is the final output. Fixation point is at the centre of the red sphere. See text for details.

A. Depth-of-field Blur

As previously discussed, variations in blur are present in retinal images of scenes containing objects at multiple depth planes. This defocus blur can prove to be an important cue to understand the distance from objects in the virtual world especially in a reaching task without the presence of haptic feedback.

A depth texture was used to create the depth map of the virtual scene. Depth information of all the vertices in the scene is stored in a Z-buffer. All depth values are scaled between 0.0 and 1.0 so that the system can be used with any HMD setting. The amount of blur associated with each pixel can be varied based on this depth information. Objects in the scene that are at the accommodative distance are kept in high acuity while smoothing is applied to all other areas of the frame.

The amount of blur depends on how far each object is from the plane of fixation (see Fig. 2). Blur can be defined as the diameter of the circle C over which the distant point Z_1 is imaged at the retina when the lens is focused at distance Z_0. This circle is referred to as the circle of confusion in the field of optics. C can be defined using the formulation developed by [20] by (1):

$$C = As\left|\frac{1}{Z_0} - \frac{1}{Z_1}\right| \quad (1)$$

where A is the aperture and s is the posterior nodal distance (distance of the lens from the retina).

The size of C can be seen as a representation for the parameter of the smoothing filter, and is directly related to the diameter of the circle of confusion ($\sigma_d \propto C$). Using this assumption, we formulate (2) for the calculation of σ_d for the defocus blur:

$$\sigma_d = K\left|\frac{1}{d_0} - \frac{1}{d_1}\right| \quad (2)$$

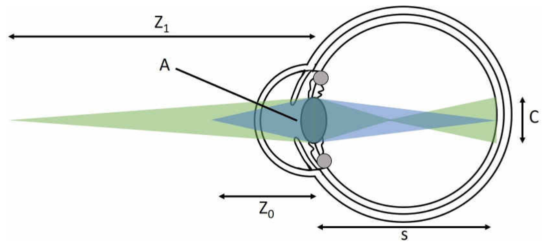

Fig. 2. When an eye is fixating at distance Z_0, the amount of blur associated with an object located at a distance Z_1 is measured with the diameter of the circle of confusion C, where A denotes the aperture and s the nodal distance.

where d_0 is the depth of the pixel under fixation, d_1 is the depth of the pixel being rendered and parameter K is the fitting of As and the constant relating C and σ_d.

An example usage of this depth-of-field effect can be seen in Fig. 1. The top image shows the source image while the middle left image shows the DoF effects. The plane of fixation is on the red sphere. All pixels at the same depth plane appear sharp. The brown cube being at the same depth plane also appears sharp. However, the outline of the red sphere is slightly blurred and it is seen as an artifact. This is due to the presence of the blurred blue cube behind it which is at a different depth plane.

B. Multi-region Foveation

Humans have foveal and peripheral vision [21]. Foveal vision is sharp and detailed while the peripheral vision lacks fidelity. Fig. 3 highlights the basic divisions in the human visual system. The central 5° constitutes the foveal region. This region has high fidelity since the light rays reaching the eye from this region form a sharp image on the retinae, whereas the fidelity decreases towards periphery due to density decrease of light sensitive cells. The peripheral regions can be broadly divided into three sections: near, mid and far peripheral regions. The further the region is from the center, the lower the fidelity is. Far peripheral region is the region which is visible to one eye and not to the other. Due to the spatial limitations of modern HMDs, far peripheral region is not visible in VR displays and is not considered.

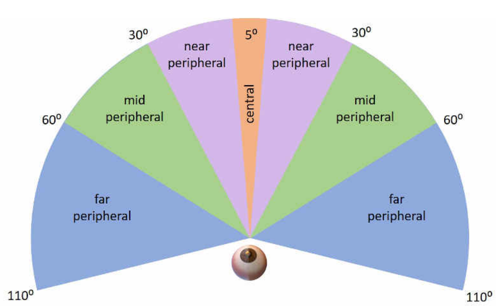

Fig. 3. Human field of view for both eyes showing the near, mid and far peripheral regions and the central (foveal) region.

In our system, the overall view is divided into three sections. The reference center of the image is the fixation point and all regions are drawn around it. The central high acuity region is output to the frame buffer without any further processing. Smoothing filter is applied to all the remaining pixels with σ_f depending on the location of the pixel. For the mid peripheral regions, σ_{f_m} is defined as 2x the σ_{f_n} of the near peripheral region.

An example output from the multi-region foveation is shown in the middle right image in Fig. 1. The fixation point is at the center of the red sphere. The central region is sharp as compared to the other regions. The external region has a lower acuity with regards to the middle circular region.

C. Artifact Removal

It can be observed that artifacts exist in the outputs of the two effects which can be uncomfortable for the user in its current form. Different techniques have been proposed in the literature to remove such artifacts. Perry and Geisler devised a technique to blend multiple resolution images based on a transfer function of the resolution map [22]. We adapted their technique to our system in order to blend the regions with abrupt σ variations. Instead of using the resolution map transfer functions, we based the blending function on the radial distance from the fixation point to the pixel currently being rendered.

We define regions as $i = 1, 2, 3$ with 3 representing the innermost region. R_i and R_{i-1} are the radii of the transitional regions where $R_i < R_{i-1}$. The magnitude of these radii depends on the resolution of the HMD and on the measure of visual eccentricity. $R(x, y)$ is the distance between the rendered pixel coordinates and the pixel coordinates of the fixation point. Let $B(x, y)$ be the blending function and is defined by (3):

$$B_i(x,y) = \begin{cases} 0 & R(x,y) \leq R_i \\ \frac{R(x,y)-R_i}{R_{i-1}-R_i} & R_i < R(x,y) < R_{i-1} \\ 1 & R(x,y) \geq R_{i-1} \end{cases} \quad (3)$$

As the rendered pixel moves closer to the inner circle, the value of the blending function approaches 0 and likewise approaches 1 when the pixel is closer to the outer limit of the transitional region. For pixels where the blending function is between 0.0 and 1.0, the output image is given by (4) where $I_i(x, y)$ and $I_{i-1}(x, y)$ are the outputs from the smoothing filters from i^{th} and $(i-1)^{th}$ regions. This way a percentage from each level is taken to form the output in the transitional regions:

$$O(x,y) = B_i(x,y)I_i(x,y) + (1 - B_i(x,y))I_{i-1}(x,y) \quad (4)$$

D. Foveated Depth-of-field Effects

The last step is to combine the two effects. We compute σ for both effects at each pixel but only use the minimum of the two values (see (5)) for the smoothing filter:

$$\sigma_p = min(\sigma_d, \sigma_f) \quad (5)$$

Example output from the combined effect can be seen in the bottom image in Fig. 1. The transition between the sharp foreground object and the blurred background is smooth with no artifacts within the 20° of eccentricity.

E. Frame Rate Comparison

To better understand the computational load required to process the rendered image, we did a comparison with the blur effect available in Unity. HTC Vive Pro Eye HMD which has an integrated Tobii eye tracking system was used. Eye tracker data was utilized to compute the fixation points. Some random scenes were played in a Unity environment and their corresponding frame processing times were observed. We also used the scenes without any blur effect applied as the reference for comparison.

Table I shows the average processing times required for each frame using the different systems considered. Our frame rate is comparable with the frame rate of the Unity blur. It should be noted that the Unity blur only applies the DoF effect, whereas our system applies two different blur processes and thus, it has better performance.

TABLE I
FRAME RATE COMPARISON.

System	Average Processing Time	Frame Rate
No Effect	$15.9ms$	$63Hz$
Unity Blur	$17.2ms$	$58Hz$
Ours	$16.7ms$	$60Hz$

IV. EXPERIMENTAL STUDY

In order to better understand the influence of using foveated DoF effects, an experimental study was carried out. The objective of this study was to understand whether the blur effect helps perceive scene depth better.

The system was implemented using Unity 3D operating on an Intel Core i7-9700K processor equipped with a NVIDIA GeForce GTX 1080 graphics card. HTC Vive Pro device, which has a resolution of 1440 x 1600 pixels per eye and a 110° field-of-view, was used for interacting with the user.

Twelve subjects, aged from 18 to 38 years (mean 27.91 $\pm$ 6.49), completed the experiment, one of whom is an author of this paper. The participants were volunteers and received no reward. All subjects had normal to corrected-to-normal acuity and normal stereo vision. Four of the subjects were fairly familiar with VR devices while the remaining had never used a VR device before.

A. Experimental Setup and Procedure

Objects of various sizes and shapes were placed on a table in the virtual scene. Fig. 4 shows the top-view of the scattered objects on the observation table. The subjects were positioned at a fixed distance from the table and were given an option to perform the experiment while either sitting on a chair or standing.

The reference object was indicated with a bright yellow spotlight to draw attention of the user. The users were given 4 seconds to observe the scene, then they were asked "how many objects are at the same depth of the reference one?". The subjects were then asked to indicate their answer by selecting a number on a virtual keypad integrated into the scene using a laser pointer attached to the HTC Vive Pro controller (see Fig. 5).

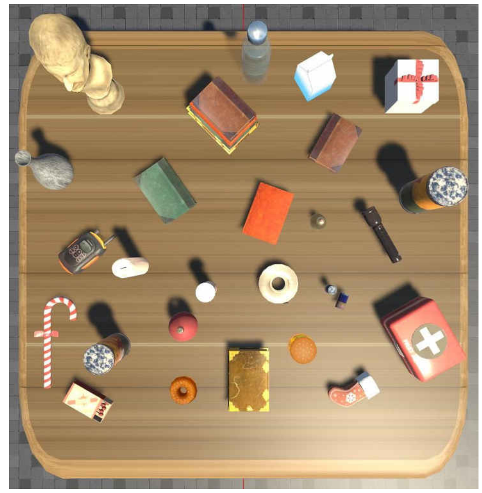

Fig. 4. Top view of the randomly placed objects to be observed.

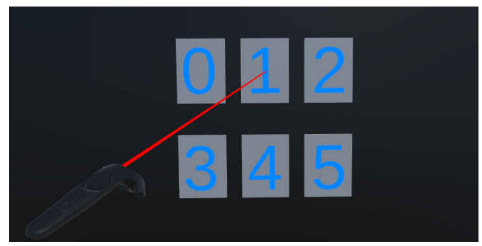

Fig. 5. Keypad display used to obtain answers from the test subjects.

Fig. 6 shows a sketch of a trial. The user is positioned approximately 2m from the table. Objects to be observed on the table are shown in colored circles and squares. The red square is the reference object while the green objects are the ones placed at the same scene depth as the reference object. The user has to look at the red square and perceive how many other objects are at the same distance from the user. In this scenario, the correct answer is 2.

Each user performed three sessions with each session having 30 trials. In each session, 15 trials were without the foveated DoF effect and 15 with the blur enabled. The sequence was random, as a result the two conditions are switched randomly during the experiment, not introducing any bias. Likewise, for each session, the order of reference objects was also randomly generated without repetition. User answers for depth perception were recorded for qualitative evaluation.

After completing the experiment, the subjects were asked to fill a subjective questionnaire in order to evaluate their experience with using the system. The open questionnaire was composed of the following questions:

- **Q1)** Do you feel any kind of dizziness after using the system?
- **Q2)** Did you notice any artifacts while changing the fixation point / were the transitions from blur to sharp and vice versa smooth?

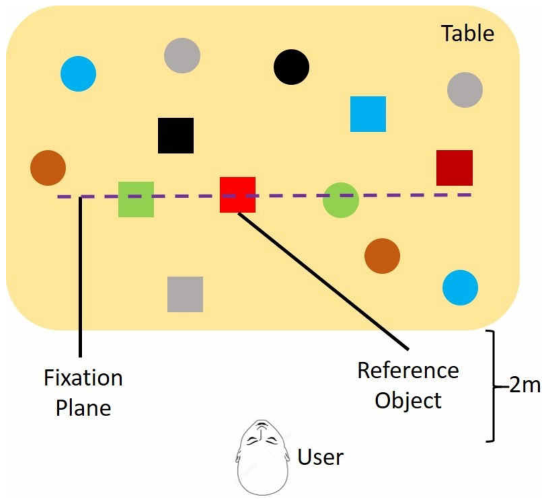

Fig. 6. A sketch of the test scenario. Colored squares and circles are the objects to be observed (see Fig. 4 and 5 for the actual virtual scene observed).

- **Q3)** Which system was more realistic/immersive?
- **Q4)** Which system do you prefer for depth perception?

B. Experimental Results

The main objective parameter to determine user performance is the accuracy of the perceived depth during each trial. We computed the true distances of each object from the user view point in each session and compared it with answers provided by the user. The number of trials where the user answered correctly is summarized in Table II: the proposed system provides a better depth perception. It can be noted that depth perception in virtual environments is not an easy task as compared to the real world.

TABLE II
ACCURACY OF EACH USER.

User	Blur Disabled	Blur Enabled
AT	6.7%	17.8%
CB	17.8%	20.0%
DG	28.9%	31.1%
GB	4.4%	17.8%
KK	11.1%	26.7%
KM	20.0%	24.4%
RH	20.0%	31.1%
RK	4.4%	26.7%
TK	22.2%	33.3%
YK	31.1%	35.6%
NZ	8.9%	13.3%
NF	15.6%	20.0%
Overall	15.9%	24.8%

We further investigated the user responses by calculating the error in their outputs. The error function we used was the mean absolute average. Performance of each user can be seen in Fig. 7. Comparing the errors between the trials with blur disabled and enabled, we observed that the performance either improved considerably or stayed the same. User performance did not deteriorate for any subject. Two of the users (GB and RK) had a high error reduction in their output.

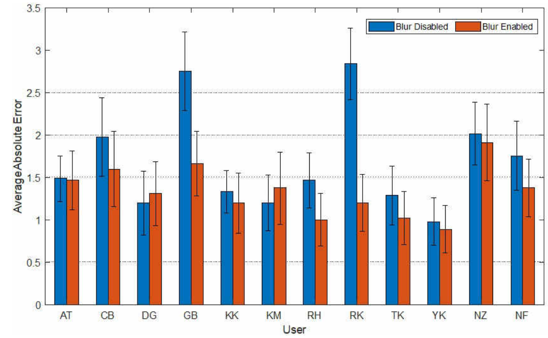

Fig. 7. Mean absolute error with its standard deviation for each subject.

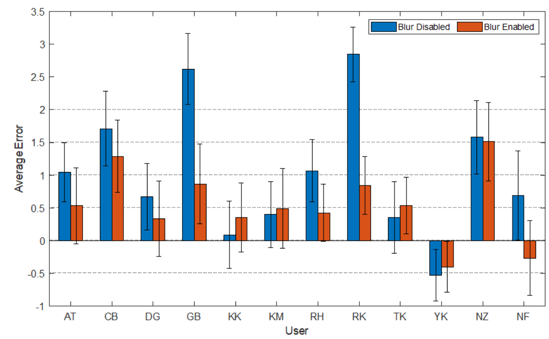

Fig. 8. Mean error with its standard deviation for each user.

In order to understand whether the user output was biased towards one side (giving a lower output than the true value or vice versa), we compared the user performance by computing the mean error (see Fig. 8). Most of the users were overestimating the objects at the same scene depth, i.e., they gave a higher answer than the true value.

A comparison of the combined performance of the subjects is presented in Table III. An overall error reduction of approximately 27% for depth perception was observed.

TABLE III
COMBINED ERROR FOR ALL THE USERS.

Error	Blur Disabled	Blur Enabled
Mean Absolute	1.69 ± 0.20	1.33 ± 0.09
Average	1.04 ± 0.33	0.54 ± 0.18

C. Observations

User opinion gathered through the post experiment questionnaire is summarized below.

Generally, users found the transitions smooth and did not perceive any noticeable artifacts. Ten of the users preferred the system with blur enabled. One user (KM) indicated that sometimes the blur provided a distraction while another (DG) indicated that the blur caused confusion in completing the tasks. It should be noted that none of the subjects except two knew what the purpose of the blur effect was or how it was calculated prior to completion of the experiment.

Only 1 user (KM) indicated about feeling a minor headache after using the system though he was slightly nauseous before using the system as well. None of the other users felt any such symptoms. One user (GB) who was familiar with VR devices found the blur enabled system to be more realistic and provided with a better sense of immersion.

Due to the random arrangement of objects, in some trials a few smaller objects were occluded by bigger objects placed in the line of sight. The test subjects were unable to notice their presence. Similarly, sometimes the user had to move his/her head to bring the reference object into focus, as a result, some objects were out of the field-of-view. Also, distance range has a subjective bias and varies from user to user. Some users may identify one nearby object to be at the same depth while others might consider the distance to be much higher than their perceived fixation plane. All these factors accounted for some of the errors in the user performance.

V. Conclusions

Our work aimed to develop a system for VR devices that mimics the real world visual experience. For this purpose, we need to take into account the limited field-of-view of VR devices and the near eye displays. True depth perception is hard in such systems. Defocus blur is an important cue for depth in the real world, however, none of the modern VR systems provide such feature. Foveated rendering is an actively researched area in the field of VR. It aims to reduce the computational load by reducing the spatial resolution in the user's periphery. We developed a system that combines depth-of-field blur and foveated imaging techniques to provide a more realistic virtual environment.

The developed system used a smoothing filter to blur the peripheral regions and the objects out of the fixation plane. Pixel-wise parameters for the filter were computed in a three step process. The first step computed the blur parameters based on the circle of confusion concept in optics. The second step divided the virtual images into multiple circular regions centered on the gaze direction of the user. Each region was assigned a different level of sharpness. In the last step, both set of parameters were combined. A blending function was incorporated into the system for removing the artifacts in the regions with abrupt changes in the sharpness. In order to have real-time capabilities, we implemented the system at the shader level using a four-pass shader.

We investigated the usefulness of our system by conducting a pilot experiment. We asked users to identify the number of objects placed at the same depth with respect to a reference object. The participants had to perform this perception task both with and without the blur effects. We observed a 27% reduction in the error of the perceived depth by incorporating our foveated DoF effects.

Acknowledgment

The authors would like to thank all the people who voluntarily participated in the experimental study.

References

[1] W. S. Geisler, "Visual Perception and the Statistical Properties of Natural Scenes," in Annu. Rev. Psychol., vol. 59, no. 1, pp. 167–192, 2008.
[2] M. A. Cohen, D. C. Dennett, and N. Kanwisher, "What is the Bandwidth of Perceptual Experience?," in Trends Cogn. Sci., vol. 20, no. 5, pp. 324–335, 2016.
[3] G. Maiello, M. Chessa, F. Solari, and P. J. Bex, "Simulated disparity and peripheral blur interact during binocular fusion," in J. Vis., vol. 14, no. 8, pp. 13:1–13:14, 2014.
[4] G. Maiello, M. Chessa, F. Solari, and P. J. Bex, "The (In)Effectiveness of Simulated Blur for Depth Perception in Naturalistic Images," in PLOS ONE, vol. 10, no. 10, pp. 10:1–10:15, 2015.
[5] F. Danieau, A. Guillo, and R. Doré, "Attention guidance for immersive video content in head-mounted displays," in 2017 IEEE Virtual Reality, Los Angeles, CA, USA, 2017, pp. 205–206.
[6] B. Bastani, E. Turner, C. Vieri, H. Jiang, B. Funt, and N. Balram, "Foveated Pipeline for AR/VR Head-Mounted Displays," in Inf. Display, vol. 33, no. 6, pp. 14–35, 2017.
[7] A. Patney, M. Salvi, J. Kim, A. Kaplanyan, C. Wyman, N. Benty, D. Luebke, and A. Lefohn, "Towards Foveated Rendering for Gaze-tracked Virtual Reality," in ACM Trans. Graph., vol. 35, no. 6, pp. 179:1–179:12, 2016.
[8] X. Meng, R. Du, M. Zwicker, and A. Varshney, "Kernel Foveated Rendering," in Proc. ACM Comput. Graph. Interact. Tech., Jul. 2018, pp. 5:1–5:20.
[9] N. T. Swafford, J. A. Iglesias-Guitian, C. Koniaris, B. Moon, D. Cosker, and K. Mitchell, "User, Metric, and Computational Evaluation of Foveated Rendering Methods," in Proc. ACM Symp. Applied Perception, Anaheim, CA, USA, 2016, pp. 7–14.
[10] R. T. Held, E. A. Cooper, J. F. O'Brien, and M. S. Banks, "Blur and Disparity Are Complementary Cues to Depth," in Curr. Biol., vol. 22, no. 5, pp. 426–431, 2012.
[11] G. Maiello, M. Chessa, B. J. Bex, and F. Solari, "Near-optimal combination of disparity across a log-polar scaled visual field," in PLOS Comput. Biol., vol. 16, no. 4, pp. 1–28, 2020.
[12] D. M. Hoffman, Z. Meraz, and E. Turner, "Sensitivity to Peripheral Artifacts in VR Display Systems," in SID Symp. Dig. Tech. Papers, vol. 49, no. 1, pp. 858–861, 2018.
[13] N. Padmanaban, R. Konrad, T. Stramer, E. A. Cooper, and G. Wetzstein, "Optimizing virtual reality for all users through gaze-contingent and adaptive focus displays," in Proc. Nat. Acad. Sci., vol. 114, no. 9, pp. 2183–2188, 2017.
[14] P. J. Bos, L. Li, D. Bryant, A. Jamali, and A. K. Bhowmik, "Simple Method to Reduce Accommodation Fatigue in Virtual Reality and Augmented Reality Displays," in SID Symp. Dig. Tech. Papers, vol. 47, no. 1, pp. 354–357, 2016.
[15] E. Turner, H. Jiang, D. Saint-Macary, and B. Bastani, "Phase-Aligned Foveated Rendering for Virtual Reality Headsets," in 2018 IEEE Conf. Virtual Reality and 3D User Interfaces, Los Alamitos, CA, USA, 2018, pp. 1–2.
[16] K. Carnegie and T. Rhee, "Reducing Visual Discomfort with HMDs Using Dynamic Depth of Field," in IEEE Comput. Graph. Appl., vol. 35, no. 5, pp. 34–41, Sep., 2015.
[17] S. Hillaire, A. Lécuyer, R. Cozot, and G. Casiez, "Depth-of-Field Blur Effects for First-Person Navigation in Virtual Environments," in IEEE Comput. Graph. Appl., vol. 28, no. 6, pp. 47–55, 2008.
[18] M. Weier, T. Roth, A. Hinkenjann, and P. Slusallek, "Foveated Depth-of-field Filtering in Head-mounted Displays," in Proc. 15th ACM Symp. Appl. Perception, Vancouver, BC, Canada, 2018, pp. 18a:1–18a:1.
[19] R. Hussain, F. Solari, and M. Chessa, "Simulated foveated depth-of-field blur for virtual reality systems," presented at ACM Eur. Conf. Vis. Media Prod., London, UK, 2019. [Online]. Available: https://www.cvmp-conference.org/files/2019/short/24.pdf
[20] R. T. Held, E. A. Cooper, J. F. O'Brien, and M. S. Banks, "Using Blur to Affect Perceived Distance and Size," in ACM Trans. Graph., vol. 29, no. 2, pp. 19:1–19:16, 2010.
[21] H. Strasburger, I. Rentschler, and M. Jüttner, "Peripheral vision and pattern recognition: A review," in J. Vis., vol. 11, no. 5, pp. 13:1–13:82, 2011.
[22] J. S. Perry and W. S. Geisler, "Gaze-contingent real-time simulation of arbitrary visual fields," in Proc. SPIE: Human Vis. Electron. Imag. VII, vol. 4662, pp. 57–69, 2002.